THE ASTRONOMICAL JOURNAL VOLUME 113, NUMBER 5 MAY 1997

ASTROMETRIC QUALITY OF THE USNO CCD ASTROGRAPH (UCA)

N. ZACHARIAS[1]
U.S. Naval Observatory, 3450 Massachusetts Avenue N.W., Washington D.C. 20392
Electronic mail: nz@pyxis.usno.navy.mil

Received 1996 December 18; revised 1997 January 27

ABSTRACT

The USNO 8-inch astrograph has been equipped with a Kodak 1536×1024 pixel CCD since 1995 June, operating in a 570–650 nm bandpass. With 3-minute exposures well exposed images are obtained in the magnitude range $R \approx 8.5 - 13.5^{m}$. An astrometric precision of 10 to 15 mas for those stars is estimated from frame-to-frame comparisons. External comparisons reveal an accuracy of about 15 mas for those stars in a 20′ field of view. For fainter stars, the error budget is dominated by the S/N ratio, reaching ≈100 mas at $R = 16^{m}$ under good observing conditions. © *1997 American Astronomical Society.*
[S0004-6256(97)01505-7]

1. INTRODUCTION

Originally the USNO 8-inch Twin Astrograph was equipped with 2 lenses corrected for the blue and visual bandpasses respectively. The instrument has been used for observing the TAC (Twin Astrographic Catalog), a northern hemisphere photographic catalog (Douglass & Harrington 1990, Zacharias *et al.* 1996) and secondary reference stars for the Radio-Optical Reference Frame (RORF) project (Zacharias *et al.* 1995) in the southern hemisphere. In 1993 the blue lens was replaced by a state-of-the-art 5-element lens, which is corrected for a 550 to 710 nm red spectral bandpass (Vukobratovich *et al.* 1993). The yellow (visual) lens is now used only for guiding with an SBIG ST4 autoguider, which moves on an x,y stage in a 2×2 degree field of view (FOV). Since 1995 June a Kodak 1536×1024 pixel CCD camera with a 9 μm pixel size has been used as a detector. The option for photographic plates has not been lost and the CCD camera can easily be exchanged with a plate holder. This instrument is now called the USNO CCD Astrograph (UCA) and currently is located on the Washington D. C. grounds of the U. S. Naval Observatory. Table 1 gives details about the telescope optics and Table 2 about the CCD camera. Currently the telescope is being upgraded to automate the observing (Germain 1996).

Preliminary results of the CCD astrometry achieved with this instrument have been reported by (Zacharias & Rafferty 1995) and (Zacharias 1996a). Here, we will investigate the astrometric precision and accuracy in more detail, including external comparisons. Section 2 describes the observations and reductions, results are presented in Sec. 3, and Sec. 4 describes methods of quality control for routine operation and future options.

[1]With Universities Space Research Association (USRA), Division of Astronomy and Space Physics, Washington D.C.

2. OBSERVATIONS AND REDUCTIONS

2.1 Focusing

The focus of the instrument depends mainly on temperature and temperature gradients, both spatial and temporal. Particularly during the cooling down period after opening the dome, frequent determinations of the correct focus setting are required for optimal results, because it cannot be predicted with sufficient accuracy. Half a dozen probes measure the air and telescope temperature at various places. The strongest correlation of focus was found with the telescope backend tube temperature. Focus changes of 0.2 mm/hour have been observed. After 2 to 3 hours of observing the focus often stays constant even if the temperature is still dropping further. The tolerance in focus setting in good seeing is about 0.05 to 0.10 mm based on CCD frame reduction results.

Various methods for focusing have been tested. Finally, a Hartmann screen technique has been adopted for routine use. A screen with 2 circular apertures of 37 mm in diameter separated by 180 mm is placed in front of the lens. A single CCD frame is taken with multiple intra- and extrafocal 10 second exposures on a 6th magnitude star, shifting the detector columns between exposures. The separation of the "double star" on the resulting frame is highly correlated with the focus setting. A linear least-squares fit reveals the location of the intersection of the rays with a formal error of about 0.02 mm. The location of the holes in the Hartmann screen are chosen to represent the full aperture "best" focus.

2.2 Data Acquisition

Most of the guided CCD frames used for this analysis were taken with 3 minute exposure times. The detector is thermoelectrically cooled to about −30 °C and stabilized to within 0.1 °C. The background is not dominated by dark current but by the bright Washington D. C. sky. Except for some tests, no diffraction grating was used until August 96. Most frames were taken within 1.5 hours of the meridian

 0004-6256/97/113(5)/1925/8/$10.00

TABLE 1. Parameters of the telescope optics.

diameter of front lens	240	mm
clear aperture	206	mm
focal length	2057	mm
plate scale	100	″/mm
filter, Schott	OG550	in front
number of lens elements	5	
spectral bandpass of lens	550–710	nm
Airy disc diameter (610 nm)	15	μm
usable flat field of view	≈9	degree diameter

TABLE 2. Parameters of the KAF 1600 CCD camera.

number of pixels	1536 × 1024	
pixel size	9.0	μm
pixel scale	0.9	″/pixel
field of view	23 × 15	arcmin
spectral bandpass used	570–650	nm
readout	16	bit
readout noise	13	e^-
dark current	0.3	e^- / pixel / sec
full well capacity	85,000	e^-
operating temperature	≈−30	C
limiting magnitude	R≈16.0	3 min. in DC

with the astrograph on the east side of the pier. The frames are stored as FITS files on a 386 PC-AT after a 16 bit A/D conversion, which takes about a minute.

In order to obtain a high star density, the frames for this analysis were taken close to the galactic plane. Fields from the radio-optical reference frame (RORF) project (Zacharias *et al.* 1995) were selected. For the regular program, a mosaic of 3-by-3 frames shifted by about 5′ was taken centered on each radio source.

2.3 Raw Image Processing

Images were transferred to an HP workstation for processing. A utility program purges the least significant bit of the pixel data, which is then stored as 2 byte signed integers with a 15 bit dynamic range. The IRAF 2.10.4 software was used for the raw data processing. The object frames were corrected only for dark current, which includes the bias. No flat fields were applied to the data. Preliminary tests with flat fields revealed no significant advantage for the astrometric results. SAOimage was used for image display and visual inspection.

Approximate instrumental magnitudes were determined from the integral signal as part of the astrometric reduction. A few photometric standard fields (Landolt 1992) were taken to determine the offset between the instrumental and photometric R magnitudes in order to estimate the limiting magnitude.

2.4 Astrometric Frame Reduction

A preliminary version of the Software for Analysing Astrometric CCD's (SAAC) (Winter 1997) was used for the detection of objects and image profile fits. Image detection is based on a minimum number of 3 consecutive pixels, each of which exceeds a threshold (S/N=3) above the background. No attempt was made to identify and retrieve faint stellar images close to the background level.

Full two-dimensional Gaussian profiles were used as image models in nonlinear least-squares adjustments. A variable aperture size was used for the profile fit, depending on the brightness of the star using about 15 to 50 pixels with equal weights. Details of the fit algorithm are described elsewhere (Winter 1997). Positions are based on a circular symmetric profile function (5 parameters). A second two-dimensional Gaussian fit was performed using an elliptical profile with 7 parameters (Schramm 1988)

$$I(x,y)=B+I_0\exp\left(\frac{-0.5}{1-\rho^2}\left[\left(\frac{x-x_0}{r_x}\right)^2+\left(\frac{y-y_0}{r_y}\right)^2-2\rho\left(\frac{x-x_0}{r_x}\right)\left(\frac{y-y_0}{r_y}\right)\right]\right),$$

where B=background level, I_0=amplitude, x_0,y_0=centroid position, r_x,r_y=radii of the profile width along the major and minor axes, and ρ=orientation. The orientation parameter ρ is in the range of +1 to −1 and is the tangent of the angle between the direction of r_x and the x-axis. Either r_x or r_y can be the major axis. The elliptical fit model is formulated this way because of a larger numerical stability than is provided by other formulas. The circular symmetric model is obtained by setting $\rho=0$ and $r_x=r_y$. Results from more advanced image profile modelling will be presented by (Winter 1997).

Double stars were not handled properly at this point. Large fit residuals or aborted fits were associated with double stars. All those stars were simply discarded from the following analysis. Galaxies were handled the same way, although down to about 15th magnitude there are not many galaxies.

Stars from overlapping frames of each field have been matched by x,y position only, using the *a priori* knowledge of the approximate frame offsets. Frame-to-frame transfor-

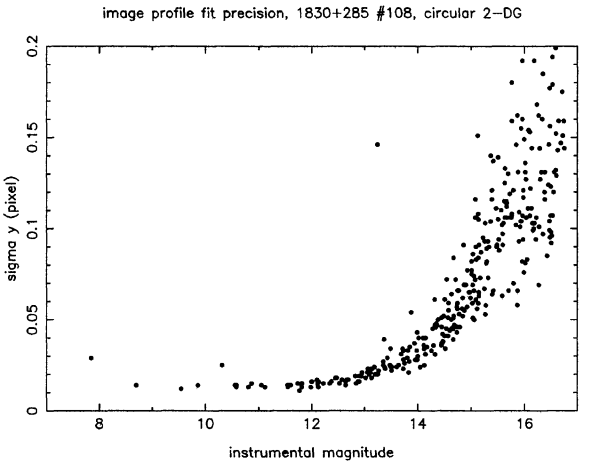

FIG. 1. Image profile fit precision along the y-axis vs instrumental magnitude for a single CCD frame taken with the USNO CCD astrograph of the field 1830+285 with a 3 minute exposure. The results are from a two-dimensional Gaussian fit. The saturation limit is at about 8.5^m. Results along the x-axis are nearly identical.

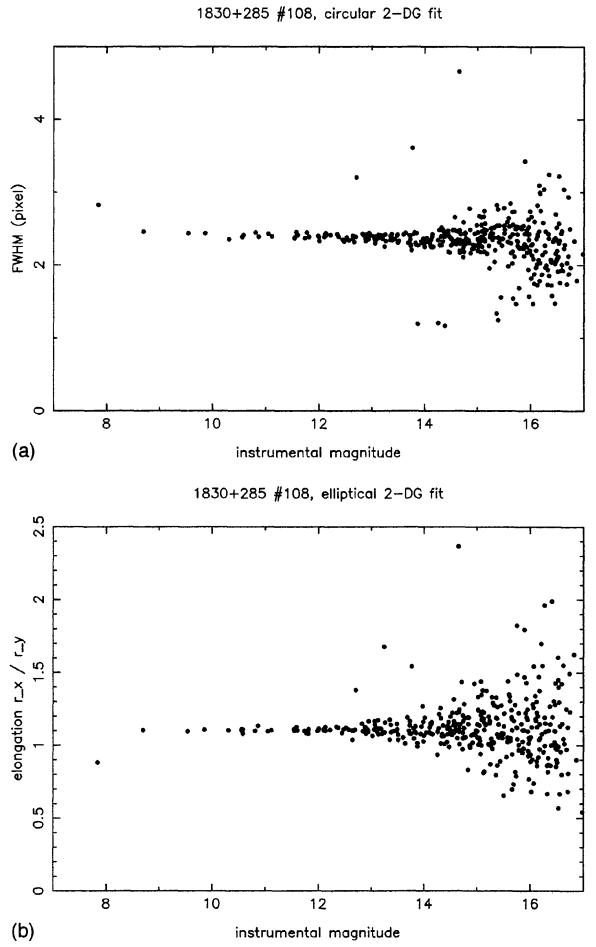

FIG. 2. The image profile full width at half maximum, FWHM (a) and image elongation (b) is displayed vs instrumental magnitude for all images of a single CCD frame. Single stars form a narrow, well-defined strip, and other objects such as double stars, galaxies or defects are clearly separated in these diagrams.

mations were performed on the x,y data using various models (offset only, orthogonal and full linear, distortion term, etc.) in least-squares adjustments. Weights were assigned to each stellar image as a function of the profile fit precision plus a constant global noise added for all images of a frame, which depends on the exposure time. This allows for the effects of atmospheric turbulence on differential astrometric observations (e.g., Zacharias 1996b).

For an external comparison, some CCD frames at small zenith distances were reduced to the celestial reference frame (right ascension, declination) using high precision reference star positions. A linear model was used for these reductions and no corrections for refraction were made, because of the smallness of the FOV. No corrections for differential color dispersion were made because of the narrow bandpass used and the small zenith distances ($\leq 30°$) of the observations.

3. ASTROMETRIC RESULTS

3.1 Image Profile Fit Precision

The image profile fit x,y-position precision, σ_{pf}, is a function of the magnitude of the stars (Fig. 1). For faint stars

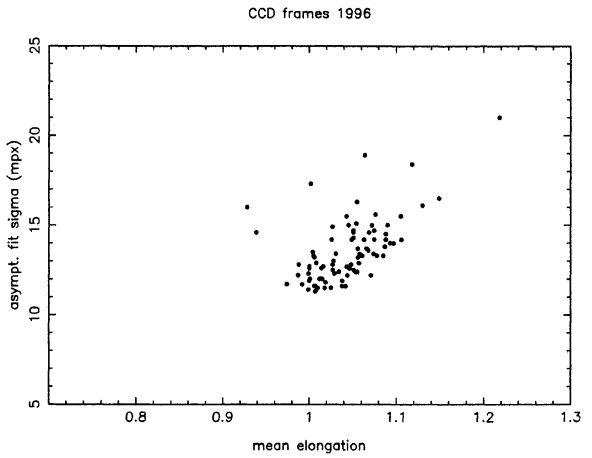

FIG. 3. The asymptotic image profile fit error, σ_{pfa}, in milli-pixels is displayed vs the mean image elongation as defined in the text. One dot represents one CCD frame. Results from CCD frames taken between 1996 January and 1996 July are shown.

the signal-to-noise ratio is the dominating error contribution. There is an asymptotic limit, σ_{pfa}, for the fit precision of bright stars. Saturated (overexposed) star images again display larger σ_{pf} simply because the assumed model function no longer resembles the observed image profile. The saturation limit for the 3-minute exposure CCD frame of Fig. 1 is about 8.5^m on the instrumental magnitude scale, which is close to the photometric R system.

The usable dynamic range, from the saturation limit to an arbitrary limit in $\sigma_{pf} = 0.1$ pixel is about 7 magnitudes. The shape and properties of the σ_{pf} vs magnitude plot does not change with exposure time, and it even remains the same for other telescopes (Zacharias *et al.* 1995). A theoretical explanation for this fact is given by (Winter 1997).

Images with significantly larger σ_{pf} than the average for a given magnitude are from double stars or galaxies or include defects in their fit area. Most of these images also show profile widths or image elongation significantly larger than the average values for a given frame, which are well defined for stars in the 8 to 15 magnitude range [Figs. 2(a) and 2(b)]. Elongation is defined as the ratio of the 2 axes (r_x/r_y) describing the image profile width radius in the elliptical Gaussian fit.

The limit in the fit precision for this CCD frame is σ_{pfa} $=0.014$ pixel $=0.13$ μm $=13$ mas for a single star image in each coordinate. Figure 3 displays σ_{pfa} vs mean image elongation for all accepted CCD frames taken between 1996 January and July for various projects. The two parameters are clearly correlated and σ_{pfa} values as low as 0.011 pixel $=10$ mas are observed.

3.2 Frame-to-Frame Transformations

A total of 29 overlapping frames was taken of the radio-optical reference frame fields 0059+581, 1830+285, and 2201+315 in 3 nights. The overlap between two frames ranged from 40 to 90% and the actual offsets from the central field were generated by random numbers for 1830+285

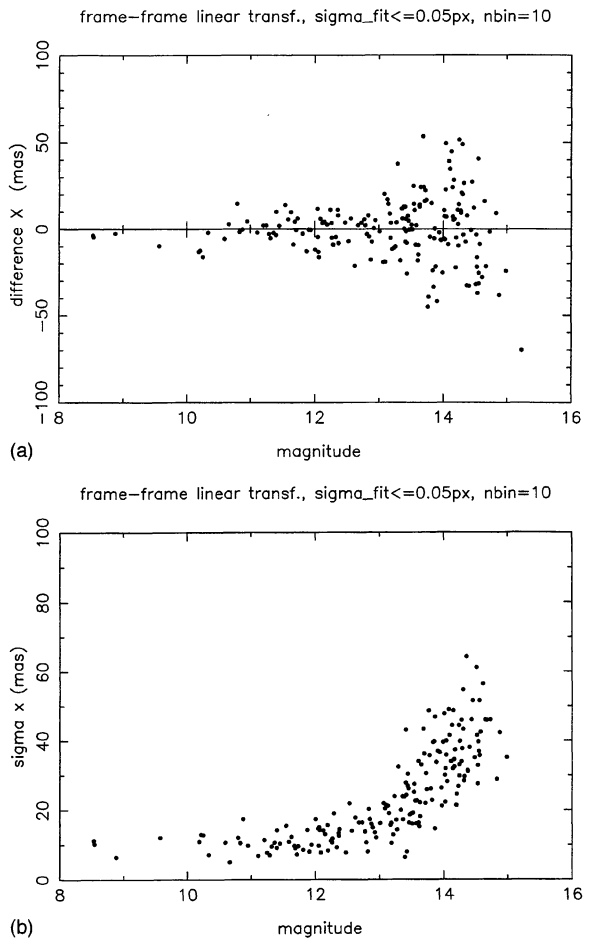

FIG. 4. Position differences (a) and corresponding standard errors (b) from frame-to-frame transformations displayed vs instrumental magnitude. In this example results from 29 overlapping frames of 3 fields are shown. Only stars with a fit error of 0.05 pixels or smaller are used. Each plot point is the average of 10 individual differences.

and 2201+315 and a regular mosaic in the case of 0059 +581. Only stars with a profile fit precision of $\sigma_{pf} \leqslant 0.05$ pixels were selected. The x,y data of each overlap frame were mapped onto the central frame of each field using a linear transformation model in a weighted least-squares adjustment. The positions, x_c, y_c and x_t, y_t from the central and the transformed overlapping frames of each star in the overlap area of those 2 frames were compared. The unweighted differences for all stars of all frame pairs in our sample are displayed in Fig. 4(a) for the x-axis vs instrumental magnitude. No significant systematic errors as a function of magnitude were yet detected. An estimate of the standard error, σ_{ff}, for a single observation per coordinate from the frame-to-frame transformation is derived from these individual differences, using $\bar{x}=(x_c+x_t)/2$ and n=2 in our case,

$$\sigma_{ff}=\sqrt{\frac{\Sigma_{i=1}^{n}(x_i-\bar{x})^2}{n-1}}=\sqrt{\frac{(x_c-x_t)^2}{2}}.$$

The data were binned, and averages of σ_{ff} are plotted vs instrumental magnitude in Fig. 4(b). A limit of σ_{ff} of 10 mas

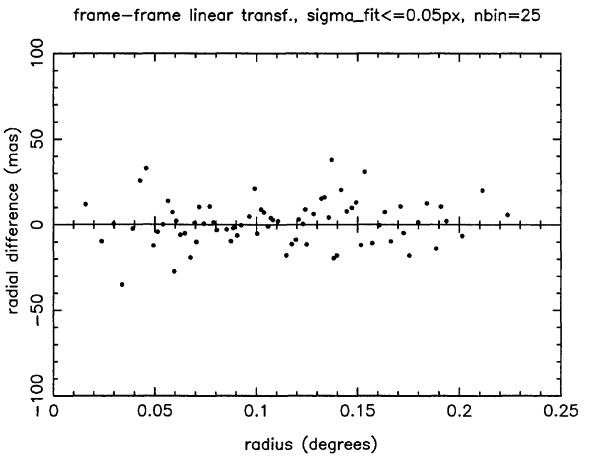

FIG. 5. Radial differences are plotted vs distance from the frame center (radius). The data were taken from the same frames as the previous figure. Each plot point is the average of 25 individual differences.

is found for well exposed stars in the 9 to 13 magnitude range. The limit obtained for σ_{ff} from frames taken on the same field center are sometimes even below 10 mas. Frames of the same field taken on different nights also show the same results. As long as the frames are well guided and in focus, there are no nightly variations in these differential astrometric observations.

3.3 Systematic Errors

No significant systematic errors (exceeding about 10 mas rms added noise) have yet been found with good CCD frames. The radial residuals vs magnitude plots show no systematic errors. Likewise no significant coma term was found in the data so far. Guiding is a problem at this level of accuracy and causes noticeable elongated images for a significant fraction of the data. Only well guided frames were used for this analysis. A more detailed investigation about possible smaller magnitude-dependent systematic errors is planned which will require much more data, the use of a grating in front of the lens and a comparison of frames taken with the telescope on different sides of the pier as well as flipping the orientation of the camera with respect to the telescope backend.

Figure 5 shows radial differences plotted vs distance from the frame center. The data were taken from the example explained in the previous section. There is no indication of a third-order optical distortion term in any of the data taken so far. This is expected because of the known small distortion of the lens and the small field of view used with the CCD. A detailed field distortion pattern analysis is not feasible yet because of the lack of a sufficient number of external reference stars (Zacharias 1995). Plots of residuals in x and y vs x and y of the fields analyzed for this paper showed no significant field distortion pattern.

3.4 External Comparison to M44 Praesepe

A high precision subset was selected from the astrometric standard field of the star cluster M44 (Russell 1976, 1986).

TABLE 3. Results of external comparisons with M44 data.

CCD frame number	number of stars	$(B-V)$ range	σ_{CPA} (mas)
65	23	0.21–1.08	41.1
66	21	0.21–1.08	42.4
65	17	0.42–0.91	38.8
66	16	0.42–0.91	38.9

Two frames of the central section of M44 were taken with the CCD astrograph (unfortunately over 2 hours from the meridian). A conventional plate adjustment (CPA) was made with the CCD frames x,y data using only stars with image profile fit errors smaller than 0.04 pixels = 36 mas. The average precision in the x,y coordinates for those stars is 18 mas. The average mean formal error of the reference stars selected from the M44 catalog for this adjustment was 25 mas per coordinate for the epoch of the CCD observations. Results from the unweighted CPA solutions are summarized in Table 3. Using the full set of stars, the standard errors of the CPA was found to be 41 and 42 mas for the 2 frames, respectively. Assuming the error estimates for the M44 reference stars are correct, and there are no systematic errors, we derive a mean accuracy $\sigma_{ext}=33$ mas for the UCA observations from this external comparison.

No corrections for refraction as a function of color were made. Most of the M44 standard field observations were made in the blue and visual spectral bandpass and systematic errors as a function of magnitude and color are suspected in those data (Russell, private communication). Our CCD observations were made in a red spectral bandpass. The 23 reference stars selected for our example have a color index in the range $B-V = 0.21$ to 1.08. The CPA was repeated with a reduced list of 17 stars with $B-V = 0.42$ to 0.91. The standard error of the adjustment dropped to just below 39 mas for both CCD frames. This corresponds to an upper limit of $\sigma_{ext}=30$ mas for our CCD observations.

3.5 External Comparison to FASTT data

A field of about 20′ around 2201+315 was observed in 1996 September with the Flagstaff Astrometric Scanning Transit Telescope (FASTT) (Stone *et al.* 1996) in 3 nights, providing 3 independent scans. In the same month 14 acceptable CCD frames were taken with the UCA with random overlaps between 40% and 90% with respect to the central frame. Only 67 well exposed stars in the magnitude range of $V=9-14$ were selected for this comparison ($\sigma_{pf}\leqslant 0.02$ pixel). The positions of the individual FASTT scans were projected onto a tangential plane to obtain ξ,η coordinates. An internal precision of $\sigma_{FASTT}=19$ mas was estimated by a linear transformation of the ξ,η between individual scans. An internal precision of $\sigma_{ff}=14$ mas was estimated from frame-to-frame transformations between x,y coordinates of individual UCA frames with the same linear model. The same linear model was used for unweighted conventional plate adjustments (CPA) of the UCA frames x,y data with 22 to 43 reference stars per frame taken from individual FASTT scans. Individual results are given in Table 4. A mean standard error of $\sigma_{CPA}=25.9$ mas was obtained. From the scatter

TABLE 4. Results of external comparisons with FASTT data.

CCD frame number	number of stars	σ_{CPA1} (mas)	σ_{CPA2} (mas)	σ_{CPA3} (mas)
236	40	25.2	27.9	23.0
237	30	22.0	22.8	20.4
238	26	21.3	24.4	21.4
239	27	22.9	24.9	18.1
240	27	25.5	27.7	23.4
241	22	27.3	31.5	24.6
242	28	30.0	31.1	20.2
243	38	29.2	35.9	25.8
244	33	33.1	23.9	22.9
247	39	27.5	25.1	25.7
248	27	25.1	24.3	21.9
249	43	26.8	29.1	25.2
250	42	26.6	28.3	23.5
251	42	31.5	30.5	29.7

of individual σ_{CPA} values in Table 4 a formal error of less than 1 mas on the mean σ_{CPA} is estimated. The quadratic sum of the internal errors of both instruments alone accounts for 24 mas of σ_{CPA}, leaving an additional noise component of only about 10 mas for any possible systematic errors in this external comparison. Figure 6 shows the CPA $\Delta\delta$ residuals of all 14 UCA frame adjustments with reference stars from the third FASTT scan as an example.

4. DISCUSSION

4.1 Why Is It So Good ?

Our CCD observations are on the 15 mas level of accuracy. With the same 2-meter focal length type of instrument about 80 mas was achieved photographically (Zacharias *et al.* 1994). There are several reasons which explain the improvement in this somewhat unfair comparison. Most of all, the photographic plates used in this comparison typically cover a FOV of several degrees while our CCD is limited to only about 20′. Thus errors introduced by the turbulence of the atmosphere, the telescope optics and geometric stability of the detector are expected to be much larger in the larger

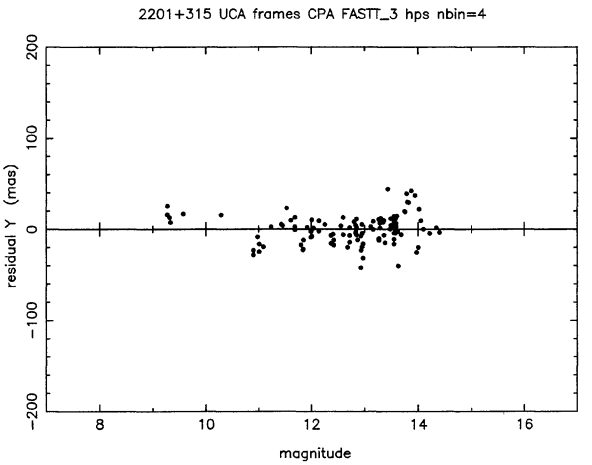

FIG. 6. Residuals of $\Delta\delta$ (y-coordinate) of conventional plate adjustments of 14 UCA frames reduced with FASTT reference stars are plotted vs V magnitude. Each plot point is the average of 4 individual residuals.

FOV, regardless of the type of detector used. Furthermore, for the above mentioned photographic results grainy emulsions were used in order to avoid anticipated problems with the hyping-process. This gives a relatively large image centering error, and recent results with fine grain emulsions show a dramatic increase in accuracy for the photographic technique (Winter & de Vegt, private communication). Finally, there is still no plate measuring machine in operation which gives an accuracy of 0.15 μm (15 mas here) over the entire plate area.

The UCA optics is a 5-element design of the 1990's and probably the best lens in the world for this type of astrometry. Observations presented in this paper utilize a tiny spot near the optical axis in a narrow bandpass. Astrometric results on the 0.015 pixel level of precision are common with modern CCD observations (e.g., Monet *et al.* 1992), where accuracies on the same level have been achieved in narrow field parallax work as well. This paper describes the first step toward wide-field astrograph-type CCD astrometry.

4.2 Where Is The Limit ?

The asymptotic limit in the profile fit error, $\sigma_{\rm pfa}$, to some extent simply reflects the difference between the model function and the real data point spread function (PSF). This can be seen in radial profile plots of the pixel data with the fit model function overlayed. A more realistic model function would lead to smaller residuals in the profile fit and thus to smaller numbers in the centroiding precision error estimate. Therefore $\sigma_{\rm pfa}$ is only an upper limit for the estimate of the measuring precision of a star's x,y coordinates, for well exposed stars the positions are better than its formal error indicates. This explains why in a frame-to-frame transformation the repeatability of the observations for centrally overlapping frames, $\sigma_{\rm ff}$, is sometimes even less than $\sigma_{\rm pfa}$. The $\sigma_{\rm ff}$ values already include the error contribution from the atmospheric turbulence, $\sigma_{\rm atm}$ in addition to the *real* fit precision of the image profiles. For our exposure time and field size we estimate $\sigma_{\rm atm} \approx$ 5 to 10 mas (Zacharias 1996b). This implies that for centrally overlapping frames the UCA performs close to the limit as set by the atmosphere for these 3-minute exposures.

Results from not centrally overlapping frames give a larger $\sigma_{\rm ff}$. This is an indication of systematic errors as a function of the location of the images in the focal plane. This is not surprising on a level of 10 mas, which is only 0.1 μm in the focal plane. Inhomogeneities in the filter, for example, could cause such effects, as well as tilt of the CCD chip with respect to the focal plane. More data need to be taken to construct a field distortion pattern (FDP), but in general a large fraction of such systematic errors can be removed by empirical calibration.

External comparisons showed the accuracy of the UCA observations to be about 15 mas for well exposed stars under optimal conditions (good seeing, close to zenith, 20′ FOV). This is in agreement with the precision of the x,y data obtained from overlapping frames. Results obtained in the M44 field do not contradict the FASTT comparison result when allowing for realistic systematic errors in the photographic data. The dynamic range for well exposed stars is about 5

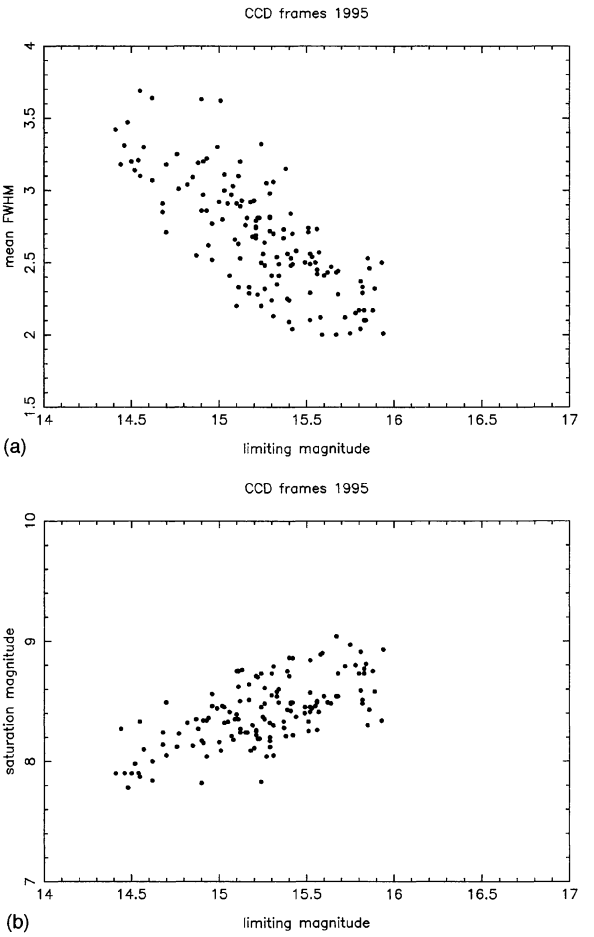

FIG. 7. The mean FWHM (a) of a CCD frame and the saturation magnitude (b) are plotted vs the limiting magnitude of each frame for all frames taken with the UCA in 1995.

magnitudes with the UCA. The S/N ratio decreases rapidly for fainter stars, limiting the precision and accuracy for a single observation to about 100 mas at about $7^{\rm m}$ below the saturation limit. In the future, comparisons with the Tycho catalog (Høg *et al.* 1995) and the Hamburg observatory data (Winter 1997) are planned.

4.3 Quality Control

The sampling with about 2 to 3 px/FWHM makes it easy to identify cosmic ray events, galaxies and most double stars [see Fig. 2(a)] with post-fit parameters like image profile width and elongation. These parameters also allow for a quantitative quality control of the data. Additional software calculates global statistics over each CCD frame for mean FWHM and mean elongation of bright but not saturated star images, limiting magnitude and magnitude at saturation level. In a second step plots of these data for several plates, e.g., the output of a night or year of observing, can be visualized and tolerances can be set for accepting good data. An example has been presented in Fig. 3.

Figure 7(a) shows the strong correlation between the lim-

iting magnitude, here defined as the magnitude where $\sigma_{pf}=0.1$ pixels, and the mean FWHM. On average, good seeing (and focusing) allows going deeper with the same exposure time. A change of the FWHM from 2.0 to 2.5 pixels results in a loss of 0.5 magnitudes for astrometry of faint stars. The saturation magnitude of a CCD frame is correlated with the limiting magnitude [Fig. 7(b)]. Deeper frames have a saturation limit shifted to fainter magnitudes as well but not by the same Δm. The dynamic range usable for astrometry is wider for deep frames, which are those with a smaller FWHM according to Fig. 7(a). No correlation of image elongation or FWHM has been found with hour angle. The orientation of images from frames with a significantly large mean image elongation was found to be always close to the x-axis (right ascension).

4.4 Future Options

A 4k CCD camera, covering a full square degree, has been obtained for this telescope. The planned USNO CCD Astrometric Catalog (UCAC-S) will cover the entire southern hemisphere in a 2-fold overlap in less than 2 years (Gauss *et al.* 1996). A grating in front of the lens will extend the dynamic range towards brighter stars to include about 90% of the Hipparcos stars using block adjustment techniques (Zacharias 1992). Based on the results of this paper an accuracy of better than 20 mas is expected for stars in the 6 to 14 magnitude range, with positional errors increasing to 70 mas for $R=16$. Additional long exposure frames in selected fields will allow a direct tie to the extragalactic reference frame (Zacharias 1997), going about 2^m fainter. Simultaneous observations of the RORF sources with larger telescopes are highly desirable to strengthen the tie.

With accuracies on the 15 mas level, parallaxes of a large number of field stars become an issue. With 8k CCDs, which are already on the horizon, giving a $2^\circ \times 2^\circ$ FOV, a complete hemisphere could be observed within about 42 nights (5000 frames, 15 frames/hour, 8 hours/night). Repeating this 5 times a year for 3 years would allow solving for positions, parallaxes and proper motions of about 10 million stars at the 10 mas level or below. This assumes that systematic errors are not larger than with the currently used small 1k CCD chip. Upcoming tests with the 4k chip will give much more insight into this issue.

5. CONCLUSION

Internal precisions of 10 to 15 mas per coordinate for a single observation have been obtained with the UCA instrument. For the first time a meaningful external accuracy estimate could be obtained by a comparison with FASTT data. Accuracies on the 15 mas level have been found in agreement with the overall error budget, leaving an additional error contribution of no more than about 10 mas for systematic errors. More data are required to investigate possible systematic errors below that level. This amazingly good result for a 2-meter focal length telescope is partly due to the high quality of the instrument and the narrow spectral bandpass, but is also a consequence of the small (20′) FOV currently used. Accurate guiding in order to obtain perfectly round images is the biggest challenge for the observing procedure. Software for quality control is in place to run a global sky catalog project, which is planned to start in the southern hemisphere in summer 1997. A direct link to the Hipparcos stars, as well as extragalactic sources, is possible. Observations with the UCA can basically replace The Tycho Catalog (ESA 1997) at current epochs. Together with the Tycho, TAC and AC (Astrographic Catalogue) data proper motions on the 2 mas/yr level could be derived for stars to about 12th magnitude. All stars of the Guide Star Catalog could be observed with 50 mas accuracy or better.

L. Winter and C. de Vegt, Hamburger Sternwarte, are thanked for providing a preliminary version of the SAAC program package, as well as R. Stone, USNO Flagstaff, for providing FASTT data of a test field. The author wishes to acknowledge T. J. Rafferty, M. E. Germain, and the instrument shop of the USNO under the supervision of J. Pohlman for maintaining and upgrading the instrument, as well as the Astrometry Department under direction of F. S. Gauss for support of this project. T. E. Corbin, M. E. Germain, and D. Pascu are thanked for valuable discussions and comments. National Optical Astronomy Observatories (NOAO) is acknowledged for IRAF, Smithsonian Astronomical Observatory for SAOimage and the California Institute of Technology for the pgplot software.

REFERENCES

Douglass, G. G., & Harrington, R. S., 1990, AJ, 100, 1712
ESA 1997, The Tycho Catalogue, ESA SP-1200
Gauss, F. S., Zacharias, N., Rafferty, T. J., Germain, M. E., Holdenried, E. R., Pohlman, J. W., & Zacharias, M. I. 1996, BAAS (in press), also http://aries.usno.navy.mil/ad/ad.html
Germain, M. E. 1996, Proceedings of the Lowell workshop on Small Telescopes, to be published on the WWW at www.noao.edu
Høg, E. 1995, A&A, 304, 150
Landolt, A. U. 1992, AJ, 104, 340
Monet, D. G., Dahn, C. C., Vrba, F. J., Harris, H. C., Pier, J. R., Luginbuhl, C. B., & Ables, H. D. 1992, AJ, 103, 638
Russell, J. L. 1976, dissertation, University of Pittsburgh, PA
Russell, J. L. 1986, in Astrometric Techniques, IAU Symp. No.109, edited by H. K. Eichhorn and R. J. Leacock (Reidel, Dordrecht), p. 697
Schramm, K. J. 1988, dissertation, University of Hamburg
Stone, R. C., Monet, D. G., Monet, A. K. B., Walker, R. L., Ables, H. D., Bird, A. R., & Harris, F. H. 1996, AJ, 111, 1721
Vukobratovich, D., Valente, T., Shannon, R. R., Hooker, R., & Summer, R. E. 1993, Report of the Optical Science Center (University of Arizona, Tucson)
Winter, L. 1997, dissertation, University of Hamburg, in preparation
Zacharias, N. 1992, A&A, 264, 296
Zacharias, N., de Vegt, C., Winter, L., & Weneit, W. 1994, in Astronomy from Wide-Field Imaging, Proceedings of the IAU Symposium 161, edited by H. T. MacGillivray, E. B. Thomson, B. M. Lasker, I. N. Reid, D. F. Malin, R. M. West, and H. Lorenz (Kluwer, Dordrecht), p. 285
Zacharias, N. 1995, AJ, 109, 1880
Zacharias, N. 1996a, BAAS, 28, 1186

Zacharias, N. 1996b, PASP, 108, 1135
Zacharias, N. 1997, in New Horizons from Multi-Wavelength Sky Surveys, IAU Symp. No. 179, edited by B. McLean (in press)
Zacharias, N., & Rafferty, T. J. 1995, BAAS, 27, 1320
Zacharias, N., de Vegt, C., Winter, L., & Johnston, K. J. 1995, AJ, 110, 3093
Zacharias, N., Zacharias, M. I., Douglass, G. G., & Wycoff, G. L. 1996, AJ, 112, 2336